

Published in final edited form as:

Sci Signal. 2011 September 20; 4(191): ra60. doi:10.1126/scisignal.2002221.

A Synthetic Biology Approach Reveals a CXCR4-G₁₃-Rho Signaling Axis Driving Transendothelial Migration of Metastatic Breast Cancer Cells

Hiroshi Yagi¹, Wenfu Tan^{1,2}, Patricia Dillenburger-Pilla¹, Sylvain Armando³, Panomwat Amornphimoltham⁴, May Simaan¹, Roberto Weigert⁴, Alfredo A. Molinolo¹, Michel Bouvier³, and J. Silvio Gutkind^{1,*}

¹Oral and Pharyngeal Cancer Branch, National Institute of Dental and Craniofacial Research, National Institutes of Health, Bethesda, MD 20852, USA

³Department of Biochemistry, Institute for Research in Immunology and Cancer, Université de Montréal, Montréal, Québec, H3C3J7, Canada

⁴Intracellular Membrane Trafficking Unit, Oral and Pharyngeal Cancer Branch, National Institute of Dental and Craniofacial Research, National Institute of Health, Bethesda, MD 20852, USA

Abstract

Tumor cells can co-opt the pro-migratory activity of chemokines and their cognate G protein-coupled receptors (GPCRs) to metastasize to regional lymph nodes or distant organs. Indeed, the migration toward SDF-1 (stromal cell-derived factor-1) of tumor cells bearing CXCR4 [chemokine (C-X-C motif) receptor 4] has been implicated in the lymphatic and organ-specific metastasis of various human malignancies. Here, we used chimeric G proteins and GPCRs activated solely by artificial ligands to selectively activate the signaling pathways downstream of specific G proteins, and showed that CXCR4-mediated chemotaxis and transendothelial migration of metastatic basal-like breast cancer cells required activation of members of the G $\alpha_{12/13}$ G protein family and of the small guanosine triphosphatase Rho. Multiple complementary experimental strategies, including synthetic biology approaches, indicated that signaling-selective inhibition of the CXCR4-G α_{13} -Rho axis prevents the metastatic spread of basal-like breast cancer cells.

INTRODUCTION

The success of therapeutic approaches that interfere with the function of HER2/Neu (also known as ErbB2, a member of the epidermal growth factor receptor family) or of the estrogen receptor has markedly reduced breast cancer mortality. However, ~15% of breast cancers are diagnosed as “triple-negative”—they lack estrogen receptors, HER2/Neu, and progesterone receptors, and thus do not respond to these targeted therapies (1, 2). 90% of breast cancer deaths stem from the metastatic spread of these triple negative breast cancers, which are often referred to as basal-like based on gene expression profiles, or from the metastatic spread of hormone receptor- or HER2/Neu-positive breast cancers with intrinsic or acquired resistance to treatment (1-4). Elucidating the mechanisms by which breast cancer cells spread from their primary sites to distant organs may identify therapeutic targets to prevent metastasis and is thus an area of intense investigation. Breast cancers metastasize preferentially to the bone, lungs, liver, and brain, and this organ-specific metastasis often

*Correspondence: sg39v@nih.gov; Telephone: (301) 496-6259; FAX: (301) 402-0823.

²Current Address: Department of Pharmacology, School of Pharmacy, Fudan University, Shanghai 201203, China

involves the aberrant expression of chemokine receptors in cancer cells concomitant with the release of chemokines from secondary organs [reviewed in (5, 6)]. Chemokines promote the migration of leukocytes to sites of inflammation, and also direct the trafficking of hematopoietic stem cells, lymphocytes, and dendritic cells between the blood and the primary and secondary lymphoid organs [reviewed in (7)]. Thus, tumor cells may gain and co-opt this pro-migratory activity of chemokines and their heterotrimeric guanine-nucleotide binding protein (G protein)-coupled receptors (GPCRs) to metastasize to regional lymph nodes and distant organs.

CXCR4 [chemokine (C-X-C motif) receptor 4] is the chemokine receptor most often implicated in breast cancer metastasis (8). Increased abundance of CXCR4 in breast cancer cells is associated with enhanced metastatic potential, and organs that are the most frequent sites of breast cancer metastasis, including the lymph nodes, lung, bone marrow, and liver, secrete the CXCR4 ligand CXCL12/SDF-1 [Chemokine (C-X-C motif) ligand 12, also known as stromal cell-derived factor-1](7, 8). Inhibiting CXCR4 with blocking antibodies and small molecule inhibitors prevents metastatic spread in model systems in which breast cancer cells are introduced into the circulatory system by intravenous or intracardiac injection (8, 9). However, whether CXCR4 is required for the initial steps of tumor cell intravasation and dissemination from the primary tumor site has been unclear. Moreover, CXCR4 antagonists promote the mobilization of hematopoietic stem cells (HSC) from the bone marrow into the peripheral blood, an effect that has hampered the exploration of CXCR4 blockers as an adjuvant for breast cancer therapy (10). Here, we show here that, in contrast to its function in HSC, which is mediated by heterotrimeric G proteins of the G_i family (11), CXCR4-initiated motility and transendothelial migration in metastatic breast cancer cells requires the activation of the small GTPase Rho through heterotrimeric G proteins of the $G_{\alpha_{12/13}}$ family. Furthermore, we show that interfering with the activation of Rho, a key molecule regulating cytoskeletal changes and cell motility (12), and hence the CXCR4-Rho signaling axis prevents the spontaneous metastasis of breast cancer cells, thereby identifying potential therapeutic targets for preventing the metastatic spread of breast cancer.

RESULTS

SDF-1 acts through CXCR4 to stimulate the migration of metastatic breast cancer cell line

CXCR4 has been implicated in organ-specific breast cancer metastasis [8, reviewed in (5, 13)], and increased abundance of CXCR4 often correlates with the poor prognosis of breast cancer patients (figs. S1A and S1B). We used a panel of human mammary gland cell lines (12) to investigate how CXCR4 promotes the migration of breast cancer cells. These lines comprise nontransformed mammary gland cells, and non-metastatic or metastatic breast tumor cells, classified as of luminal or basal-like cell origin based on their gene expression signatures (14). Most cells migrated to epidermal growth factor (EGF) (15). However, although basal-like breast cancer cells are generally more motile in response to serum than are luminal cells (14), migration toward a gradient of SDF-1 was primarily observed in those basal-like cell lines shown to metastasize in animal models, the widely-used breast cancer model MDA-MB-231 (8, 14), and SUM-159 (16) (Fig. 1A). Thus, the ability of breast cancer cells to respond to SDF-1 appears to correlate with metastatic behavior. MCF-7, a luminal-ductal-derived breast cancer cell that does not metastasize in vivo, migrates in response to SDF-1, albeit less far than do MDA-MB-231 or SUM-159. Both MDA-MB-231 and SUM-159 cells migrated toward SDF-1 (Fig. 1B and fig. S1C). SDF-1 promoted the invasion of MDA-MB-231 cells into collagen gels (Fig. 1C and 1D), and the specific CXCR4 inhibitor AMD3100 prevented SDF-1 induced cell migration in a dose-dependent manner without affecting the migratory response to EGF (fig. S1D). These results support

that SDF-1 can act through CXCR4 to induce the migration of invasive basal-like breast cancer cells.

The SDF-1-CXCR4 interaction mediates transendothelial breast cancer cell migration in vitro and spontaneous metastasis of breast cancer cells to lymph nodes in vivo

Interfering with CXCR4 function prevents metastasis in experimental models involving intravenous or intracardiac delivery of breast cancer cells (8, 9, 17-19). However, for spontaneous metastasis to occur, cancer cells must first invade the surrounding tissues and enter the circulation. To explore the possible role of CXCR4 in these early events, we began by knocking down MDA-MB-231 cell CXCR4 by means of lentiviral-mediated RNA-interference. CXCR4 knock down decreased MDA-MB-231 cell migration to SDF-1 without affecting their response to EGF (Fig. 1E and 1F). Next, we investigated the passage of cancer cells through endothelial monolayers as a model of intravasation (Fig. 1G). Although SDF-1 did not disrupt endothelial barrier function as judged by the passage of high molecular weight fluorescent-labeled dextran (20), it stimulated the migration of MDA-MB-231 cells through both vascular (VEC) and lymphatic (LEC) endothelial monolayers, an effect that was inhibited by AMD3100 or by knocking down CXCR4 (Figs. 1H and 1I, and figs. S1E and S1F).

To investigate whether CXCR4 contributes to the initial steps of breast cancer metastasis in vivo, we implanted breast cancer cells into the mammary fat pad of mice, a procedure that leads to their spontaneous metastasis to the lymph nodes and secondary organs (21). MDA-MB-231 cells injected into mammary fat pad of SCID/NOD mice [a mouse model system that combines the SCID (severe combined immunodeficiency) and the NOD (non obese diabetic) models of immunodeficiency] grew at the primary site and metastasized to multiple distant sites, including locoregional and distant lymph nodes, lung, and liver (Figs. 1J-1L). Tumor cells were observed within lymphatic vessels (Fig. 1L), and, consistent with prior reports (21), 5 out of 15 mice examined (33%) displayed multiple metastatic lesions in the lungs. The weight of the invaded lymph nodes was measured for each mouse and the presence of metastatic lesions was confirmed histopathologically (Figs. 1K and 1M). CXCR4 knock down did not affect the growth of the primary tumors (figs. S1G and S1H), but markedly decreased their metastatic spread to the lymph nodes (Fig. 1M), with none of the mice in which CXCR4 was knocked down mice displaying cancerous lesions in the lung ($p < 0.05$). These findings support a critical role for CXCR4 in the early steps in breast cancer metastasis.

Activation of $G\alpha_i$ is not sufficient to promote the migration of metastatic breast cancer cells

CXCR4, like other chemokine receptors, couples to $G\alpha_i$ subunits of heterotrimeric G proteins (22). As expected, treatment of MDA-MB-231 cells with pertussis toxin (PTX), which inhibits $G\alpha_i$, decreased the phosphorylation of Akt induced by SDF-1 without affecting Akt activation by EGF (Fig. 2A). Similarly, PTX prevented the migration of the non-metastatic luminal breast cancer cell line MCF-7 toward SDF-1, reflecting the contribution of $G\alpha_i$ to migration in these cells (Fig. 2B). In contrast, PTX treatment had little effect on SDF-1-induced cell migration of MDA-MB-231 and SUM-159 cells (Fig. 2B). Similarly, transendothelial migration of MDA-MB-231 cells toward SDF-1 was not blocked by PTX (Figs. 2C and 2D), raising the possibility that G proteins in addition to, or other than, $G\alpha_i$ may participate in the biological response mediated by CXCR4 in these cells.

These observations prompted us to use a synthetic biology strategy to reconstitute G protein-regulated networks in breast cancer cells. We stably expressed a mutant $G\alpha_i$ -coupled GPCR,

called G_i RASSL (receptors activated solely by synthetic ligands), which has lost the ability to respond to its natural ligand, but gained the ability to respond to a pharmacologically inert compound, clozapine-N-oxide (CNO) (23) (Figs. 2E and 2F). CNO induced the phosphorylation of Akt in MDA-MB-231 cells expressing G_i RASSL in a PTX sensitive fashion but did not stimulate Akt phosphorylation in parental cells (Figs. 2G and 2H), as expected if G_i RASSL signals through G_{α_i} in response to CNO in these cells. However, CNO failed to induce cell migration in either experiments using mass cultures of G_i RASSL-expressing cells or experiments using sorted cell populations with abundant G_i RASSL (Fig. 2I). Similar results were obtained with HEK-293T cells expressing abundant G_i RASSL and with SUM-159 cells (see below and fig.S3D). Collectively, these data suggest that G_i activity may not be sufficient, or strictly necessary, to induce cell migration mediated by CXCR4 in metastatic breast cancer cells.

Activation of Rho is integral to the pathway by which SDF-1 promotes cell migration through CXCR4 in breast cancer cells

We next investigated whether the three prototypical Rho-family GTPases, Rho, Rac, and Cdc42, all of which have been linked to cell movement (12), were involved in CXCR4-mediated migration of metastatic breast cancer cells. SDF-1 stimulated a rapid increase in the fraction of Rho in the active GTP-bound state, reaching a maximum at ~5 min in both MDA-MB-231 and SUM-159 cells (Fig. 3A), but did not induce Rac activation, which appeared to be in the activated state prior to SDF-1 stimulation. CXCR4 knockdown decreased SDF-1-dependent activation of Akt and Rho in MDA-MB-231 cells (Fig. 3B). However, whereas in MDA-MB-231 cells Akt activation was inhibited by PTX, activation of Rho by SDF-1 was not (Fig. 3C), indicating that G_i and its G_{α_i} subunit, G_{α_i} , are not involved in CXCR4-mediated Rho activation (24). We used both transfection of siRNA targeting RhoA and treatment with C3 toxin, which ADP-ribosylates Rho and inhibits its function (25), to determine whether Rho activation is involved in the SDF-1-dependent migration of MDA-MB-231 cells. Either RhoA knockdown or treatment with C3 toxin inhibited the migration of MDA-MB-231 cells toward SDF-1 (Figs. 3D-3F). Moreover, expression of RhoA I41, a C3 toxin-resistant form of RhoA, reversed inhibition of SDF-1-dependent cell migration by C3 toxin, whereas expression of wild-type RhoA did not (Fig. 3G). Together, these data indicate that SDF-1 can activate Rho through CXCR4 independently of G_i , and that activated RhoA, in turn, contributes to SDF-1-dependent breast cancer cell migration.

$G_{\alpha_{12/13}}$ couples to CXCR4 and is necessary for SDF-1-induced human breast cancer cell transendothelial migration in vitro and metastasis in vivo

$G_{\alpha_{12}}$ and $G_{\alpha_{13}}$ ($G_{\alpha_{12/13}}$, which together define the $G_{\alpha_{12/13}}$ G protein family) and the G_{α_q} family of G protein α subunits can activate RhoA (26, 27). $G_{\alpha_{12/13}}$, encoded by the *GEP* oncogene (28, 29), is abundant in breast cancer cells (30, 31), contributes to tumor spread in a syngeneic murine breast cancer metastasis model (31), and correlates with metastatic potential (31) and poor prognosis (fig. S2A) in human patients. $G_{\alpha_{12/13}}$ promotes Rho activation by binding to the RGS domain of RGS-containing Rho guanine nucleotide exchange factors (GEFs) (32). A chimeric molecule consisting of green fluorescent protein (GFP) fused to the RGS domain of PDZ-RhoGEF, which behaves as a dominant negative mutant for $G_{\alpha_{12/13}}$, inhibited SDF-1-dependent Rho activation, as well as SDF-1-dependent invasion and migration in MDA-MB-231 cells (Figs. 3H-3M), suggesting that the $G_{\alpha_{12/13}}$ -Rho signaling axis contributes to CXCR4-mediated cell migration in breast cancer cells.

$G_{\alpha_{12}}$ and $G_{\alpha_{13}}$ are generally more abundant in human breast cancer-derived cell lines than in normal or non-tumorigenic mammary epithelial cells (Fig. 4A). In the two basal-like metastatic breast cancer cells examined (SUM-159 and MDA-MB-231), the abundance of

$G\alpha_{13}$ was high, with the protein levels of $G\alpha_{12}$ lower than in the non-metastatic SUM-149 cells. To investigate role of $G\alpha_{12/13}$ in the migration of MDA-MB-231 cells directly, we knocked down $G\alpha_{12/13}$ by stably expressing shRNAs targeting $G\alpha_{12}$ and $G\alpha_{13}$ in MDA-MB-231 cells (Fig. 4B). The activation of Rho and migration of MDA-MB-231 cells promoted by SDF-1 were both blocked by $G\alpha_{12/13}$ knock down (Figs. 4C and 4D). $G\alpha_{13}$ appears to play a more prominent role, as knock down of $G\alpha_{13}$ was sufficient to prevent breast cancer cell migration in response to SDF-1, consistent with its greater abundance in MDA-MB-231 cells. Together, our data suggest CXCR4 can couple to $G\alpha_{13}$, and possibly to $G\alpha_{12}$ in cells in which $G\alpha_{12}$ is abundant, to promote Rho activation and cell migration in response SDF-1. Furthermore, $G\alpha_{12/13}$ knock down markedly inhibited the ability of MDA-MB-231 cells injected into the mammary fat pad of SCID/NOD mice to invade the lymph nodes, with little effect on the size of the primary tumors (Figs. 4E and fig. S2B), indicating that $G\alpha_{12/13}$ and CXCR4 may play a pivotal role in the metastatic spread of breast cancer.

The ability of CXCR4 to promote chemotaxis in leukemic T cells may require both PTX-sensitive G proteins and PTX-insensitive G proteins of the G12/13 family (33). However, whether this is due to a direct effect of CXCR4 on G12/13 is unclear, as emerging evidence support a broad impact of G12/13 in immune cell function (34), while $G\alpha_{13}$ can regulate CXCR4 trafficking, hence modulating the response to SDF-1 indirectly (35) We focused on $G\alpha_{13}$, and used bioluminescence resonance energy transfer (BRET) to determine whether CXCR4 can interact directly with this G protein α subunit (Fig. 4F) (36). Indeed, BRET titration curves supported a direct CXCR4- $G\alpha_{13}$ interaction (Fig. 4G). SDF-1 significantly decreased CXCR4- $G\alpha_{13}$ BRET, indicating that receptor activation results in a conformational reorganization of the receptor-G protein complex (Fig. 4H) (36). In contrast, activation of a related chemokine receptor, CCR2, by its cognate agonist MCP-1, did not affect the marginal BRET signal between CCR2 and $G\alpha_{13}$, indicating that CXCR4 but not CCR2 selectively engaged $G\alpha_{13}$ (Fig. 4H). However, agonist-promoted changes in BRET revealed that both CXCR4 and CCR2 engaged $G\alpha_i$ (Fig. 4I). Analyses of BRET between $G\alpha_{13}$ and $G\gamma_7$ indicated that SDF-1 promoted a conformational rearrangement of the G_{13} heterotrimer in cells co-transfected with CXCR4 (figs. S2C and S2D), further supporting the activation of $G\alpha_{13}$ in the response to SDF-1. This direct interaction has functional consequences. Indeed, CXCR4 overexpression alone is not sufficient to promote the migration of transfected cells in response to SDF-1, but cells migrate readily when G_{13} is concomitantly overexpressed with CXCR4, while this manipulation does not affect the migratory response to EGF (Fig. 4J).

A synthetic biology approach reveals a key role for $G\alpha_{13}$ in breast cancer cell motility and transendothelial migration

To determine whether $G\alpha_{13}$ contributes to directed migration of breast cancer cells, we engineered a GPCR- $G\alpha_{13}$ coupled system that could be activated by an artificial ligand. . For this synthetic biology approach, we created $G\alpha_{13i5}$, a chimeric form of $G\alpha_{13}$ in which the C-terminal 5 amino acids were replaced by those of $G\alpha_i$, enabling its coupling to and activation by G_i RASSL (Fig. 5A). We tested the functional activity of this reconstituted chimeric system by examining its ability to activate Rho in HEK-293T cells (Figs. 5B and 5C). CNO activated ERK1/2 but not Rho in HEK-293T cells transfected with expression constructs encoding G_i RASSL, but when $G\alpha_{13i5}$ was co-expressed with G_i RASSL, CNO activated both Rho and ERK1/2 activation (Fig. 5C). HEK-293T cells expressing both G_i RASSL and $G\alpha_{13i5}$ migrated toward wells containing various concentration of CNO (Fig. 5D), whereas cells expressing G_i RASSL alone did not, indicating that $G\alpha_{13}$ activity is necessary to promote the migration of HEK-293T cells. Next, we engineered MDA-MB-231 cells stably expressing G_i RASSL with or without $G\alpha_{13i5}$ (Fig. 5E and figs. S3B and S3C). CNO stimulated Akt phosphorylation in cells expressing G_i RASSL, a response that was

reduced in cells expressing both G_i RASSL and $G\alpha_{13i5}$ (Fig. 5E). Co-expression of G_i RASSL and $G\alpha_{13i5}$ was sufficient to activate Rho in response to CNO (Fig. 5E and fig. S3A). Moreover, co-expression of G_i RASSL and $G\alpha_{13i5}$ was necessary and sufficient to promote the migration of MDA-MB-231 cells toward gradients of CNO in Boyden chambers and collagen gels, as well as in transendothelial migration assays (Figs. 5F-5H). Similarly, co-expression of G_i RASSL and $G\alpha_{13i5}$ was necessary and sufficient to induce the migration in response to CNO in SUM-159 cells, and in MCF-12A, a normal mammary epithelial cell line (figs. S3D-F).

We next performed a more detailed analysis of the migratory behavior induced by CXCR4 activation or through CNO activation of the G_i and G_{13} signaling networks using video microscopy and individual cell tracking (Fig. I-J). Exposure to SDF-1 increased the motility of MDA-MB-231 cells, and promoted their directional migration toward the chemokine gradient. CNO treatment enhanced the motility of MDA-MB-231 cells expressing G_i -RASSL, so that they moved at speeds comparable to or faster than that observed for MDA-MB-231 cells after CXCR4 activation. However, their movement appeared to be random; thus, the directionality of their movement was not different from that of control, unstimulated cells. In contrast, CNO stimulation of cells co-expressing G_i RASSL and $G\alpha_{13i5}$ stimulated their migration toward the agonist gradient, thereby mimicking SDF-1 activation of CXCR4. Together, our results indicate that CXCR4 coupling to $G\alpha_{13}$ and Rho is required for the directional migration and invasive properties of metastatic basal-like breast cancer cells.

Interfering with the CXCR4- $G\alpha_{13}$ -Rho signaling axis may provide a targeted approach to preventing breast cancer transendothelial migration and metastatic spread

We next asked whether the signaling pathway initiated by CXCR4- $G\alpha_{13}$ might present a suitable therapeutic target for preventing breast cancer metastasis. $G_{12/13}$ signaling activates multiple downstream molecules, including E-cadherin and β -catenin, Hax-1, Radixin, RhoGEFs, and MEK5, many of which contribute to cell motility and metastasis (37). Here, we focused on Rho kinase (ROCK), which acts downstream of Rho. ROCK promotes the accumulation of phospho-myosin light chain (pMLC) by phosphorylating MLC and inhibiting MLC phosphatase, thereby promoting cell migration by regulating actomyosin contraction (38), a process that may contribute to transcellular tumor invasion (39). SDF-1 increased the abundance of pMLC in MDA-MB-231 cells, was an effect diminished by RhoA knock down (Figs. 6A and 6B), or by the inhibition of ROCK with the ROCK inhibitors, Y27632 and fasudil (Fig. 6C). Furthermore, CNO increased pMLC abundance in MDA-MB-231 cells co-expressing G_i RASSL and $G\alpha_{13i5}$ but not those expressing G_i RASSL alone, an increase that was blocked by pretreatment with fasudil (Fig. 6D). Fasudil also prevented chemotaxis, transendothelial migration, and invasion by MDA-MB-231 cells in response to SDF-1, and in response to CNO in cells co-expressing G_i RASSL and $G\alpha_{13i5}$ (Figs. 6E-6I and figs. S4A-S4F). Moreover, fasudil markedly inhibited the metastatic spread of MDA-MB-231 cells injected into the mammary fat pads of SCID/NOD mice (Fig. 6J). Thus, the ability to interfere with CXCR4 activation of $G\alpha_{13}$ and the Rho-dependent signaling pathways downstream may represent potential targeted approaches for preventing breast cancer metastasis.

DISCUSSION

90% of breast cancer deaths occur as a consequence of metastatic disease (3, 40); thus the molecular mechanisms underlying metastasis have warranted considerable attention (4). An emerging view is that various chemokines and cytokines released by the tumor cells and their stroma provide a permissive microenvironment for tumor growth and its metastatic spread. Numerous chemokines and their GPCRs have been implicated in intercellular

communication between tumor cells, tumor-associated fibroblasts, and the multiple immune- and inflammatory-cells that constitute the complex tumor microenvironment (5, 6, 41). Tumor cells also gain the ability to migrate in response to chemokine gradients, facilitating tumor cell dissemination through the lymphatic and cardiovascular systems (7). The interaction between CXCR4 and SDF-1 has been implicated in the organ-specific metastasis of breast, prostate, and lung cancers (5, 42). Here, we show that the ability of to guide the migration of breast cancer cells requires the CXCR4 coupling to $G\alpha_{13}$, a protein that is over-expressed in metastatic basal-like breast cancer cells, and the consequent activation of the Rho signaling axis. Indeed, by reengineering G protein-regulated signaling networks in breast cancer cells using GPCRs activated by artificial ligands and chimeric G proteins, we determined that the activation of $G\alpha_{13}$ is necessary and sufficient to stimulate Rho, thereby promoting the chemotaxis, invasion, and transendothelial migration of basal-like breast cancer cells. These findings suggest that interfering with the CXCR4- $G\alpha_{13}$ -Rho signaling axis and their key downstream targets may provide previously-unexplored options to halt breast cancer metastasis.

CXCR4, like most chemokine receptors, couples to G proteins of the $G\alpha_i$ family (22). However, whereas some GPCRs exhibit a strict G-protein-coupling specificity, other GPCRs may exhibit a less restricted coupling ability, which may depend on the abundance of GPCRs, G protein α subunits, and downstream targets (5). This concept is well exemplified by the observation that CXCR4 induces cell migration in luminal-ductal-derived breast cancer cells through the activation of a pertussis toxin-sensitive mechanism involving a Rac GEF, P-Rex1, that acts as direct downstream target from G_i (15). Surprisingly, however, analysis of P-Rex1 abundance in hundreds of human breast tumor samples revealed that this Rac GEF is specifically overexpressed in estrogen-receptor-positive (ER+) and ErbB2-positive (HER2+) breast cancers, but is nearly absent in basal-like (triple negative) breast cancer tissues and their derived cell lines (15). This may explain the lack of robust activation of Rac1 in basal-like metastatic breast cancer cells in response to SDF-1, which instead appear to use a $G\alpha_{13}$ -Rho-dependent mechanism to promote cell migration and invasion. Collectively, these observations indicate that CXCR4 may deploy a pro-metastatic signaling route in basal-like breast cancers distinct from estrogen-receptor-positive (ER+) and ErbB2-positive (HER2+) breast cancers, and suggest that this specificity could perhaps be exploited for therapeutic purposes.

The coupling of CXCR4 to $G\alpha_{13}$ may also contribute to the acquisition of epithelial-mesenchymal transition (EMT)-like features that characterize the most aggressive and metastatic breast cancers (43, 44). Indeed, in addition to promoting cell migration, the heterotrimeric $G\alpha_{12/13}$ proteins activate transcription factors that control the expression of metalloproteases such as MMP-2 and MMP-9, thereby enabling tissue invasion (5), enhance cell motility by reducing cell-extracellular matrix adhesion through integrins (45), and decrease the rigidity of cell-cell contacts by reducing the stability of homophilic E-cadherin interactions (46). Thus, whereas most physiological processes controlled by CXCR4 may involve the activation of G_i -family G proteins and their signaling cascades, we can hypothesize that basal-like metastatic breast cancer cells are selected for their ability to overexpress $G\alpha_{13}$, and thus link it to CXCR4, thereby gaining the ability to activate Rho. This may increase the capacity to migrate toward SDF-1 released by secondary target organs, while contributing to the acquisition of a more motile and pro-invasive phenotype. Certainly, the metastatic process is highly complex, and thus the contribution of CXCR4 and G_{13} to each step involved in breast cancer dissemination requires further investigation. The abundance of CXCR4 may increase in the hypoxic environments often observed in solid tumors due to transcriptional activation of its promoter (47) by hypoxia-inducible factor (HIF). Alternatively, CXCR4 abundance can be enhanced by the activation of HER2/Neu and their downstream pathways, which limit CXCR4 degradation (48). Thus, preventing the

aberrant expression of CXCR4 may represent one of the mechanisms by which currently available cancer treatments targeting HER2/Neu may reduce breast cancer metastasis. CXCR4 also appears to be abundant in breast cancer tumor initiating cells or cancer stem cells (49), suggesting that the primary tumor mass may include a subpopulation of cells with increased tumor-regenerating potential that overexpress CXCR4. Thus, we can speculate that among these tumor stem cells, those overexpressing $G\alpha_{13}$ may represent “metastasis stem cells” that may already exist within the tumor mass. Alternatively, we can speculate that the CXCR4-expressing cancer stem cells that acquire the ability to overexpress $G\alpha_{13}$ may be selected through their capacity to give rise to cancer cells that become more competent to migrate, intravasate, and ultimately infiltrate and colonize the lymph nodes and secondary organs, thereby compromising patient survival.

Whereas CXCR4 inhibitors represent obvious candidates for adjuvant therapy preventing breast cancer metastasis, their specific side effects have hampered their clinical use in the preventing metastasis (10), although they have been approved by the FDA for the mobilization of hematopoietic stem cells. In fact, $G\alpha_i$ activation is required for SDF-1-CXCR4-mediated retention of hematopoietic progenitors within the bone marrow (11), suggesting that long-term inhibition of CXCR4 signaling through $G\alpha_i$ may not be clinically feasible in breast cancer patients. However, perturbing CXCR4 coupling to the $G\alpha_{13}$ family or inhibiting its downstream targets may provide a reasonable approach to preventing metastasis in patients at risk. For example, fasudil, which is currently used in the clinic for vasospasm and pulmonary hypertension (50), blocked CXCR4 and $G\alpha_{13}$ -promoted cell migration and prevented spontaneous breast cancer metastasis in the SCID/NOD mouse model. Fasudil does not mobilize hematopoietic stem cells, suggesting that the CXCR4- $G\alpha_{13}$ -Rho pathway is dispensable for their retention in the bone marrow. Similarly, various widely-used cholesterol-lowering statins can block Rho function (51), without eliciting substantial side effects, suggesting that they could be beneficial in breast cancer metastasis prevention.

Structural information for many GPCRs suggests that activated members of this family of receptors may adopt multiple conformations (52), which could, in turn, selectively engage distinct downstream signaling pathways. Different ligands can preferentially activate or inhibit subsets of the G-protein-linked signaling pathways engaged by a given GPCR (53). Whereas most of the physiological functions of CXCR4 involve the activation of $G\alpha_i$, it is becoming apparent that CXCR4 can interact physically with G_{13} , and can thereby activate Rho to promote the metastatic spread of basal-like breast cancer cells. These findings support the potential clinical benefits of developing GPCR antagonists or negative allosteric regulators that specifically prevent the activation of the $G\alpha_{12/13}$ -Rho pathway by CXCR4. Indeed, considering that GPCRs are the target directly or indirectly of more than 50% of the current therapeutic agents in the market (54), we can envision that the development of a class of signaling-selective GPCR antagonists may present a unique opportunity to control the pathological functions of GPCRs while restricting the side effects caused by disrupting their multiple physiological roles. Although more extensive animal studies may be required to define how CXCR4- $G_{12/13}$ signaling influences each step of the metastatic process, the present study provides a rationale for the future development and evaluation of $G\alpha_{12/13}$ -Rho-selective CXCR4 inhibitors for metastasis prevention.

MATERIALS AND METHODS

Cell Culture

184-A1 and MCF-12A normal mammary epithelial cell lines, MCF-10-2A non-tumorigenic mammary epithelial cell line, MCF-7, T-47D, BT-474, BT-549, and MDA-MB-231 human breast cancer cell lines and human epithelial kidney 293-T cells were purchased from

ATCC. SUM-149 and SUM-159 human breast cancer cell lines (16, 55) were purchased from Asterand. Neonatal human dermal lymphatic microvascular endothelial cells were purchased from Lonza. Immortalized human vascular endothelial cells were described previously (56). Cell lines were cultured according to manufacturers' instructions.

Transfections

Nonsilencing control RNA sequence and RhoA silencing RNA sequence (Qiagen) were transfected using the HiPerfect reagent (Qiagen).

Cell Migration and Collagen Gel Invasion Assays

Migration assays were performed using 48-well Boyden chamber with 8 μm pore size polyvinyl pyrrolidone-free polycarbonate membrane (NeuroProbe) coated with fibronectin. Cells were added to the upper chamber and chemoattractant was added to the lower chamber in serum-free DMEM. After incubation for 6 h at 37°C, cells on the upper surface of the membrane were removed and cells on the lower surface were fixed and stained. Images were taken of the entire lower surface of the membranes, and the number of migrated cells was counted (4 wells per conditions). Invading cells were visualized by confocal microscopy.

Reagents and Antibodies

Recombinant human stromal cell-derived factor 1 alpha, EGF, biotin-conjugated mouse monoclonal anti-CXCR4 antibody, and anti-mouse IgG2B isotype antibody were purchased from R&D Systems. Rabbit polyclonal anti-phospho ERK1/2, phospho Akt, Akt, phospho myosin light chain 2 myosin light chain 2 and GAPDH antibodies were purchased from Cell Signaling Technology. Rabbit polyclonal anti-ERK1/2, Rho, $G\alpha_{12}$, $G\alpha_{13}$, and α -tubulin antibodies were purchased from Santa Cruz Biotechnology. Mouse monoclonal anti-Rac1 and Cdc42 antibodies were purchased from BD Biosciences. Mouse anti-GFP and HA antibodies were purchased from Covance. AMD3100 octahydrochloride, Clozapine N-oxide, and Y-27632 dihydrochloride monohydrate were purchased from Sigma. Exoenzyme C3 and pertussis toxin were purchased from List Biological Laboratories. Fasudil was purchased from LC Laboratories.

Plasmid Constructs

Expression vectors for $G\alpha_{12}$, $G\alpha_{13}$, $G\alpha_{13i5}$, RhoA, RhoA I41, and GFP fused to the RGS domain of PDZ-RhoGEF (GFP-RGS) have been described previously (57-61). Expression vector for G_i RASSL was kindly provided by Brian Roth (62). Lentiviral vector for CXCR4 shRNA, $G\alpha_{12}$ shRNA and $G\alpha_{13}$ shRNA have been described previously (33).

Lentivirus Production and Infection

Lentiviral stocks were prepared and titrated using HEK-293T cells as the packaging cells as previously reported (61). Breast cancer cells were incubated with viral supernatants for 16 h. After that, the cells were returned to normal growth medium. Infected cells were selected with 1 $\mu\text{g}/\text{ml}$ puromycin.

Chemotaxis assay using μ -Slide

Chemotaxis was measured using the μ -Slides from ibidi (ibidi GmbH, Munich, Germany) according to the manufacturer's instructions. Briefly, the observation area of the slides was coated with fibronectin (100 $\mu\text{g}/\text{mL}$) for 1 h and then washed once with water and let dry at room temperature for 1 h. MDA-MB-231 cells expressing control plasmid, G_i RASSL, or G_i RASSL with $G\alpha$ were then incubated for 3 h at 37°C in a humid atmosphere. SDF-1 (50 ng/mL) or CNO (50 nM) were used as chemoattractants and added to the upper reservoir. Images were collected every 10 min for 24 h on a Zeiss LSM 700 confocal

microscope with a 10x objective equipped with a CO₂ and temperature controlled chamber. Data were analyzed for cell migration using Manual Tracking (<http://rsbweb.nih.gov/ij/plugins/track/track.html>), a plugin of Image J (<http://rsb.info.nih.gov/ij/>), and Chemotaxis and Migration tool from ibidi (http://www.ibidi.de/applications/ap_chemo.html). The rose diagram, which shows the distribution of migration angles, calculated from x-y coordinates at the beginning and end of the cell tracks, was also plotted, followed by the Rayleigh test to determine significant clustering of migration directions (63, 64). A significant alignment or distribution of direction migrations in the direction of the chemoattractant gradient was used to judge positive chemotaxis towards the chemoattractant (63, 64).

Collagen Gel Invasion Assay

Collagen gel invasion assay was carried out using collagen type I gels. Briefly, 500 μ l of collagen gel at the concentration of 2 mg/ml was set within a 12 mm diameter, 0.4 μ m pore filter transwell (Corning). Then 2×10^5 cells in serum-free DMEM were plated on the collagen gel, and 1 ml of DMEM supplemented with chemoattractant was applied underneath the filter. After incubation for 24 h at 37°C, collagen gel was fixed with 4% paraformaldehyde and confocal Z slices were collected from each gel.

Transendothelial Migration Assay

Immortalized human vascular endothelial cells or neonatal human dermal lymphatic microvascular endothelial cells (1×10^5) were plated onto a 6.5 mm diameter, 8 μ m pore filter transwell (Corning) coated with 10 μ g/ml of collagen type I and then incubated with complete growth medium for 4 days. The tightness of endothelial barrier was tested by in vitro permeability assay as described previously by measuring the passage of fluorescent-labeled 60 kD molecular weight dextran (20). Indeed, SDF-1 did not promote the permeability of fluorescent dextran under conditions in which the passage of this tracer in response to multiple vascular permeability factors, such as VEGF, was readily detectable (20). Breast cancer cells stably expressing GFP or RFP (2×10^5) in serum-free DMEM were seeded in the upper chamber and DMEM supplemented with chemoattractant was applied in the lower chamber. After incubation for 24 h at 37 °C, inserts were washed with PBS and fixed with 4% paraformaldehyde for 20 min. Cells on the upper membrane were removed with a cotton swab and then membranes were mounted on microscope slides. Pictures from 4 inserts per condition were taken, and the number of transmigrated cells was individually counted in each image.

Spontaneous Breast Cancer Metastasis model in SCID mouse

All animal studies were carried out according to National Institutes of Health-approved protocols, in compliance with the Guide for the Care and Use of Laboratory Animals. The spontaneous metastasis model of breast cancer cells was based on prior studies (21, 65). In brief, non-obese diabetic severe combined immunodeficient (SCID/NOD) mice at 6 weeks age were used for the in vivo metastasis assay. Wild type MDA-MB-231 cells (2×10^6) or MDA-MB-231 cells infected with control shRNA, CXCR4 shRNA, or G $\alpha_{12/13}$ shRNA were injected into mammary fat pad. Mice were sacrificed 40 days after injection and organs were collected for histological analysis. For Fasudil experiments, 20 mg/kg per day Fasudil or equal volume of PBS was administered through intraperitoneal injections at a dose.

Bioluminescence Resonance Energy Transfer (BRET)

Fourty eight hours before transfection, HEK-293T cells were plated on 96 well plates coated with poly-L-ornithine hydrobromide (Sigma Aldrich) at a density of 100,000 cells per well. Transient transfections were performed using the linear polyethylenimine (Mw 25000,

Polysciences) method, with a DNA: polyethylenimine ratio of 2:7. Thirty ng of $G\alpha_{13}$ -*RLucII* were co-transfected with either an increasing amount of CXCR4-GFP2, ranging from 20 ng to 800 ng, or with soluble GFP2, ranging from 1 ng to 100 ng, to perform the titration curves. The effect of ligands binding on conformation between receptors and $G\alpha_{13}/G\alpha_i$ was assessed at maximal BRET values for each of the conditions, with 30 ng of either $G\alpha_{13}$ -*RLucII* or $G\alpha_{i91}$ -Luc (36) and 800 ng of either CXCR4-fluorescent protein (GFP2 or venus) or 800 ng CCR2-fluorescent protein (GFP2 or venus) (66). SDF-1 or MCP-1 was added at a final concentration of 200 nM for 10 min. The ligand-induced effect between $G\alpha_{13}$ and $G\gamma_7$ was examined by cotransfecting 200 ng of non-tagged CXCR4 receptor with 30 ng of $G\alpha_{13}$ -*RLucII* and 500 ng of $G\gamma_7$ -GFP2. SDF-1 was added at a final concentration of 200 nM for 10 min. The abundance of the GFP2 or Venus-tagged energy acceptor proteins was measured as total fluorescence using a FlexStationII (Molecular Device) with excitation filters at 400 or 485 nm and emission filters at 510 or 538 nm, respectively. The abundance of the energy donor (*RLuc* and *RLucII*) tagged proteins were measured using a Mithras LB940 plate reader (Berthold Technologies, Bad Wildbad, Germany) in the presence of 5 μ M coelenterazine 400A or coelenterazine h (Biotium) for BRET2 or BRET1, respectively, after 5 min of incubation. For BRET measurements, cells were washed once 48 h after transfection with PBS and coelenterazine 400A or coelenterazine h was added to a final concentration of 5 μ M in PBS 5 min before BRET2 or BRET1 reading, respectively. Emitted light was then collected using a MITHRAS LB940 multidetector plate reader, allowing the sequential integration of the signals detected in the 480 (\pm) 20 nm and 530 (\pm) 20 nm windows for the donor and acceptor light emissions, respectively. The BRET signal was determined by calculating the ratio of the light intensity emitted by the acceptor over the light intensity emitted by the donor. The values were corrected by subtracting the background BRET signal detected when the donor construct was expressed alone.

Flow Cytometric Analysis

Cells were harvested and washed three times with phosphate-buffered saline. Following incubation with biotin-conjugated anti-CXCR4 antibody or isotype control antibody for 60 min at room temperature, the cells were treated with streptavidin-phycoerythrin-conjugated IgG (Vector Laboratories) for 30 min at room temperature and analyzed with a BD Biosciences flow cytometer.

Immunofluorescence

The following antibodies were used for tissue immunofluorescence; goat polyclonal anti-LYVE1; 1:200 (Abcam), polyclonal rabbit anti-cytokeratin, wide spectrum screening; 1:500 (Dako). Unstained 5 μ m paraffin sections were dewaxed, hydrated through graded alcohols and distilled water, and washed three times with PBS. Antigens were retrieved using 10 mmol/L citric acid in a microwave for 20 min. The slides were allowed to cool for 30 min at room temperature, rinsed twice with PBS, and immersed in 3% hydrogen peroxide in PBS for 10 min to quench the endogenous peroxidase. The sections were then sequentially washed in distilled water and PBS and incubated in blocking solution (2.5% bovine serum albumin in PBS) for 30 min at room temperature. Excess solution was discarded and the primary antibody was applied diluted in blocking solution at 4 $^{\circ}$ C overnight. After three washes in PBS, sections were incubated with fluorescein-conjugated secondary antibodies (1:100) for 1 h at room temperature in blocking buffer. Slides were then washed with PBS and mounted with Vectashield (Vector Laboratories).

Immunocytochemistry

MDA-MB-231 cells infected with control or HA-tagged G_i RASSL lentivirus were plated on the coverslips coated with 10 μ g/ml of fibronectin. After 24 h of incubation, cells were washed with ice-cold PBS and fixed with 4% paraformaldehyde in PBS. After washing three

times with PBS, cells were incubated with 10% FBS in PBS for 30 min. Fixed cells were incubated with the primary antibody (anti-HA; 1: 150) for 1 h, followed by a 45 min incubation with the secondary antibody (goat anti-mouse Alexa Fluor 488; Invitrogen). Coverslips were then mounted onto glass slides.

Immunoblot Analysis

Cells were lysed at 4 °C in lysis buffer (50 mM Tris-HCl, 150 mM NaCl, 1% Nonidet P-40) supplemented with protease inhibitors (0.5 mM phenylmethylsulfonyl fluoride, 10 µg/ml aprotinin and leupeptin). Equal amounts of proteins were subjected to SDS-polyacrylamide gel electrophoresis and transferred onto a polyvinylidene difluoride membrane (Immobilon P; Millipore). The membranes were then incubated with the appropriate antibodies.

Rho GTPase Pull Down Assay

Rho activity in cultured cells was assessed by a modified method described elsewhere (27). Briefly, after serum-starvation for 16 h, cells were treated as indicated and lysed at 4 °C in a buffer containing 20 mM HEPES, pH 7.4, 0.1 M NaCl, 1% Triton X-100, 10 mM EGTA, 40mM β-glycerophosphate, 20mM MgCl₂, 1 mM Na₃VO₄, 1 mM dithiothreitol, 10 µg/mL aprotinin, 10 µg/mL leupeptin, and 1 mM phenylmethylsulfonyl fluoride. Lysates were incubated with glutathione S-transferase (GST)–rhotekin–Rho binding domain previously bound to glutathione-Sepharose beads and washed 3 times with lysis buffer. Associated GTP-bound forms of Rho, Rac1, or Cdc42 were released with protein loading buffer and analyzed by Western blot analysis using polyclonal antibody against RhoA.

Live Cell Imaging

Live cell imaging was performed using an inverted Zeiss LSM 700 confocal microscopes with samples contained in glass-bottomed MatTek slides or using the µ-Slides from ibidi (ibidi GmbH, Munich, Germany).

Statistical Analysis

All experiments were repeated at least 3-4 times with similar results. Statistical analysis of migration assay, transendothelial migration assay, and the weight of primary tumors or metastases was performed by unpaired t-test. Asterisks denote statistical significance (NS, P > 0.05; *P < 0.05; **P < 0.01; and ***P < 0.001). The Rayleigh test was applied to determine significant clustering of migration directions (63, 64).

Supplementary Material

Refer to Web version on PubMed Central for supplementary material.

References

1. Weigelt B, Reis-Filho JS. Histological and molecular types of breast cancer: is there a unifying taxonomy? *Nat Rev Clin Oncol.* 2009; 6:718. [PubMed: 19942925]
2. Gluz O, Liedtke C, Gottschalk N, Pusztai L, Nitz U, Harbeck N. Triple-negative breast cancer--current status and future directions. *Ann Oncol.* 2009; 20:1913. [PubMed: 19901010]
3. Fidler IJ. The pathogenesis of cancer metastasis: the 'seed and soil' hypothesis revisited. *Nat Rev Cancer.* 2003; 3:453. [PubMed: 12778135]
4. Gupta GP, Massague J. Cancer metastasis: building a framework. *Cell.* 2006; 127:679. [PubMed: 17110329]
5. Dorsam RT, Gutkind JS. G-protein-coupled receptors and cancer. *Nat Rev Cancer.* 2007; 7:79. [PubMed: 17251915]

6. Karnoub AE, Weinberg RA. Chemokine networks and breast cancer metastasis. *Breast Dis.* 2006; 26:75. [PubMed: 17473367]
7. Balkwill F. Cancer and the chemokine network. *Nat Rev Cancer.* 2004; 4:540. [PubMed: 15229479]
8. Muller A, Homey B, Soto H, Ge N, Catron D, Buchanan ME, McClanahan T, Murphy E, Yuan W, Wagner SN, Barrera JL, Mohar A, Verastegui E, Zlotnik A. Involvement of chemokine receptors in breast cancer metastasis. *Nature.* 2001; 410:50. [PubMed: 11242036]
9. Liang Z, Yoon Y, Votaw J, Goodman MM, Williams L, Shim H. Silencing of CXCR4 blocks breast cancer metastasis. *Cancer Res.* 2005; 65:967. [PubMed: 15705897]
10. Epstein RJ. The CXCL12-CXCR4 chemotactic pathway as a target of adjuvant breast cancer therapies. *Nat Rev Cancer.* 2004; 4:901. [PubMed: 15516962]
11. Papayannopoulou T, Priestley GV, Bonig H, Nakamoto B. The role of G-protein signaling in hematopoietic stem/progenitor cell mobilization. *Blood.* 2003; 101:4739. [PubMed: 12595315]
12. Bar-Sagi D, Hall A. Ras and Rho GTPases: a family reunion. *Cell.* 2000; 103:227. [PubMed: 11057896]
13. Nguyen DX, Bos PD, Massague J. Metastasis: from dissemination to organ-specific colonization. *Nat Rev Cancer.* 2009; 9:274. [PubMed: 19308067]
14. Neve RM, Chin K, Fridlyand J, Yeh J, Baehner FL, Fevr T, Clark L, Bayani N, Coppe JP, Tong F, Speed T, Spellman PT, DeVries S, Lapuk A, Wang NJ, Kuo WL, Stilwell JL, Pinkel D, Albertson DG, Waldman FM, McCormick F, Dickson RB, Johnson MD, Lippman M, Ethier S, Gazdar A, Gray JW. A collection of breast cancer cell lines for the study of functionally distinct cancer subtypes. *Cancer Cell.* 2006; 10:515. [PubMed: 17157791]
15. Sosa MS, Lopez-Haber C, Yang C, Wang H, Lemmon MA, Busillo JM, Luo J, Benovic JL, Klein-Szanto A, Yagi H, Gutkind JS, Parsons RE, Kazanietz MG. Identification of the Rac-GEF P-Rex1 as an essential mediator of ErbB signaling in breast cancer. *Mol Cell.* 2010; 40:877. [PubMed: 21172654]
16. Valastyan S, Reinhardt F, Benaich N, Calogrias D, Szasz AM, Wang ZC, Brock JE, Richardson AL, Weinberg RA. A pleiotropically acting microRNA, miR-31, inhibits breast cancer metastasis. *Cell.* 2009; 137:1032. [PubMed: 19524507]
17. Tamamura H, Hori A, Kanzaki N, Hiramatsu K, Mizumoto M, Nakashima H, Yamamoto N, Otaka A, Fujii N. T140 analogs as CXCR4 antagonists identified as anti-metastatic agents in the treatment of breast cancer. *FEBS Lett.* 2003; 550:79. [PubMed: 12935890]
18. Smith MC, Luker KE, Garbow JR, Prior JL, Jackson E, Piwnica-Worms D, Luker GD. CXCR4 regulates growth of both primary and metastatic breast cancer. *Cancer Res.* 2004; 64:8604. [PubMed: 15574767]
19. Richert MM, Vaidya KS, Mills CN, Wong D, Korz W, Hurst DR, Welch DR. Inhibition of CXCR4 by CTCE-9908 inhibits breast cancer metastasis to lung and bone. *Oncol Rep.* 2009; 21:761. [PubMed: 19212637]
20. Gavard J, Gutkind JS. VEGF controls endothelial-cell permeability by promoting the beta-arrestin-dependent endocytosis of VE-cadherin. *Nat Cell Biol.* 2006; 8:1223. [PubMed: 17060906]
21. Dadiani M, Kalchenko V, Yosepovich A, Margalit R, Hassid Y, Degani H, Seger D. Real-time imaging of lymphogenic metastasis in orthotopic human breast cancer. *Cancer Res.* 2006; 66:8037. [PubMed: 16912179]
22. Dutt P, Wang JF, Groopman JE. Stromal cell-derived factor-1 alpha and stem cell factor/kit ligand share signaling pathways in hemopoietic progenitors: a potential mechanism for cooperative induction of chemotaxis. *J Immunol.* 1998; 161:3652. [PubMed: 9759889]
23. Conklin BR, Hsiao EC, Claeysen S, Dumuis A, Srinivasan S, Forsayeth JR, Guettier JM, Chang WC, Pei Y, McCarthy KD, Nissenson RA, Wess J, Bockaert J, Roth BL. Engineering GPCR signaling pathways with RASSLs. *Nat Methods.* 2008; 5:673. [PubMed: 18668035]
24. Rosenfeldt H, Castellone MD, Randazzo PA, Gutkind JS. Rac inhibits thrombin-induced Rho activation: evidence of a Pak-dependent GTPase crosstalk. *J Mol Signal.* 2006; 1:8. [PubMed: 17224083]
25. Kikuchi A, Yamamoto K, Fujita T, Takai Y. ADP-ribosylation of the bovine brain rho protein by botulinum toxin type C1. *J Biol Chem.* 1988; 263:16303. [PubMed: 3141405]

26. Worzfeld T, Wettschureck N, Offermanns S. G(12)/G(13)-mediated signalling in mammalian physiology and disease. *Trends Pharmacol Sci.* 2008; 29:582. [PubMed: 18814923]
27. Chikumi H, Vazquez-Prado J, Servitja JM, Miyazaki H, Gutkind JS. Potent activation of RhoA by Galpha q and Gq-coupled receptors. *J Biol Chem.* 2002; 277:27130. [PubMed: 12016230]
28. Xu N, Bradley L, Ambdukar I, Gutkind JS. A mutant alpha subunit of G12 potentiates the eicosanoid pathway and is highly oncogenic in NIH 3T3 cells. *Proc Natl Acad Sci U S A.* 1993; 90:6741. [PubMed: 8393576]
29. Xu N, Voyno-Yasenetskaya T, Gutkind JS. Potent transforming activity of the G13 alpha subunit defines a novel family of oncogenes. *Biochem Biophys Res Commun.* 1994; 201:603. [PubMed: 8002992]
30. Gutkind, JS.; Coso, OA.; Xu, N. *G Proteins, Receptors, and Disease.* S, AM., editor. Humana Press; Totowa, NJ: 1998. p. 101-117.
31. Kelly P, Moeller BJ, Juneja J, Booden MA, Der CJ, Daaka Y, Dewhirst MW, Fields TA, Casey PJ. The G12 family of heterotrimeric G proteins promotes breast cancer invasion and metastasis. *Proc Natl Acad Sci U S A.* 2006; 103:8173. [PubMed: 16705036]
32. Fukuhara S, Chikumi H, Gutkind JS. RGS-containing RhoGEFs: the missing link between transforming G proteins and Rho? *Oncogene.* 2001; 20:1661. [PubMed: 11313914]
33. Tan W, Martin D, Gutkind JS. The Galpha13-Rho signaling axis is required for SDF-1-induced migration through CXCR4. *J Biol Chem.* 2006; 281:39542. [PubMed: 17056591]
34. Herroeder S, Reichardt P, Sassmann A, Zimmermann B, Jaeneke D, Hoeckner J, Hollmann MW, Fischer KD, Vogt S, Grosse R, Hogg N, Gunzer M, Offermanns S, Wettschureck N. Guanine nucleotide-binding proteins of the G12 family shape immune functions by controlling CD4+ T cell adhesiveness and motility. *Immunity.* 2009; 30:708. [PubMed: 19409815]
35. Kumar A, Kremer KN, Dominguez D, Tadi M, Hedin KE. Galpha13 and Rho mediate endosomal trafficking of CXCR4 into Rab11+ vesicles upon stromal cell-derived factor-1 stimulation. *J Immunol.* 2011; 186:951. [PubMed: 21148034]
36. Gales C, Rebois RV, Hogue M, Trieu P, Breit A, Hebert TE, Bouvier M. Real-time monitoring of receptor and G-protein interactions in living cells. *Nat Methods.* 2005; 2:177. [PubMed: 15782186]
37. Juneja J, Casey PJ. Role of G12 proteins in oncogenesis and metastasis. *Br J Pharmacol.* 2009; 158:32. [PubMed: 19422395]
38. Amano M, Ito M, Kimura K, Fukata Y, Chihara K, Nakano T, Matsuura Y, Kaibuchi K. Phosphorylation and activation of myosin by Rho-associated kinase (Rho-kinase). *J Biol Chem.* 1996; 271:20246. [PubMed: 8702756]
39. Itoh K, Yoshioka K, Akedo H, Uehata M, Ishizaki T, Narumiya S. An essential part for Rho-associated kinase in the transcellular invasion of tumor cells. *Nat Med.* 1999; 5:221. published online EpubFeb (. [PubMed: 9930872]
40. de Boer M, van Deurzen CH, van Dijck JA, Borm GF, van Diest PJ, Adang EM, Nortier JW, Rutgers EJ, Seynaeve C, Menke-Pluymers MB, Bult P, Tjan-Heijnen VC. Micrometastases or isolated tumor cells and the outcome of breast cancer. *N Engl J Med.* 2009; 361:653. published online EpubAug 13 (. [PubMed: 19675329]
41. Orimo A, Gupta PB, Sgroi DC, Arenzana-Seisdedos F, Delaunay T, Naeem R, Carey VJ, Richardson AL, Weinberg RA. Stromal fibroblasts present in invasive human breast carcinomas promote tumor growth and angiogenesis through elevated SDF-1/CXCL12 secretion. *Cell.* 2005; 121:335. published online EpubMay 6 (. [PubMed: 15882617]
42. Zlotnik A. New insights on the role of CXCR4 in cancer metastasis. *J Pathol.* 2008; 215:211. [PubMed: 18523970]
43. Polyak K, Weinberg RA. Transitions between epithelial and mesenchymal states: acquisition of malignant and stem cell traits. *Nat Rev Cancer.* 2009; 9:265. [PubMed: 19262571]
44. Thiery JP, Acloque H, Huang RY, Nieto MA. Epithelial-mesenchymal transitions in development and disease. *Cell.* 2009; 139:871. [PubMed: 19945376]
45. Gong H, Shen B, Flevaris P, Chow C, Lam SC, Voyno-Yasenetskaya TA, Kozasa T, Du X. G protein subunit Galpha13 binds to integrin alpha11beta3 and mediates integrin "outside-in" signaling. *Science.* 2010; 327:340. [PubMed: 20075254]

46. Meigs TE, Fields TA, McKee DD, Casey PJ. Interaction of Galpha 12 and Galpha 13 with the cytoplasmic domain of cadherin provides a mechanism for beta -catenin release. *Proc Natl Acad Sci U S A*. 2001; 98:519. [PubMed: 11136230]
47. Staller P, Sulitkova J, Lisztwan J, Moch H, Oakeley EJ, Krek W. Chemokine receptor CXCR4 downregulated by von Hippel-Lindau tumour suppressor pVHL. *Nature*. 2003; 425:307. [PubMed: 13679920]
48. Li YM, Pan Y, Wei Y, Cheng X, Zhou BP, Tan M, Zhou X, Xia W, Hortobagyi GN, Yu D, Hung MC. Upregulation of CXCR4 is essential for HER2-mediated tumor metastasis. *Cancer Cell*. 2004; 6:459. [PubMed: 15542430]
49. Hwang-Verslues WW, Kuo WH, Chang PH, Pan CC, Wang HH, Tsai ST, Jeng YM, Shew JY, Kung JT, Chen CH, Lee EY, Chang KJ, Lee WH. Multiple lineages of human breast cancer stem/progenitor cells identified by profiling with stem cell markers. *PLoS One*. 2009; 4:e8377. [PubMed: 20027313]
50. Rikitake Y, Liao JK. ROCKs as therapeutic targets in cardiovascular diseases. *Expert Rev Cardiovasc Ther*. 2005; 3:441. [PubMed: 15889972]
51. Demierre MF, Higgins PD, Gruber SB, Hawk E, Lippman SM. Statins and cancer prevention. *Nat Rev Cancer*. 2005; 5:930. published online EpubDec (. [PubMed: 16341084]
52. Rosenbaum DM, Rasmussen SG, Kobilka BK. The structure and function of G-protein-coupled receptors. *Nature*. 2009; 459:356. [PubMed: 19458711]
53. Galandrin S, Oligny-Longpre G, Bouvier M. The evasive nature of drug efficacy: implications for drug discovery. *Trends Pharmacol Sci*. 2007; 28:423. [PubMed: 17659355]
54. Rajagopal S, Rajagopal K, Lefkowitz RJ. Teaching old receptors new tricks: biasing seven-transmembrane receptors. *Nat Rev Drug Discov*. 2010; 9:373. [PubMed: 20431569]
55. Flanagan L, Van Weelden K, Ammerman C, Ethier SP, Welsh J. SUM-159PT cells: a novel estrogen independent human breast cancer model system. *Breast Cancer Res Treat*. 1999; 58:193. [PubMed: 10718481]
56. Edgell CJ, McDonald CC, Graham JB. Permanent cell line expressing human factor VIII-related antigen established by hybridization. *Proc Natl Acad Sci U S A*. 1983; 80:3734. [PubMed: 6407019]
57. Crespo P, Xu N, Simonds WF, Gutkind JS. Ras-dependent activation of MAP kinase pathway mediated by G-protein beta gamma subunits. *Nature*. 1994; 369:418. [PubMed: 8196770]
58. Fukuhara S, Marinissen MJ, Chiariello M, Gutkind JS. Signaling from G protein-coupled receptors to ERK5/Big MAPK 1 involves Galpha q and Galpha 12/13 families of heterotrimeric G proteins. Evidence for the existence of a novel Ras AND Rho-independent pathway. *J Biol Chem*. 2000; 275:21730. [PubMed: 10781600]
59. Marinissen MJ, Chiariello M, Tanos T, Bernard O, Narumiya S, Gutkind JS. The small GTP-binding protein RhoA regulates c-jun by a ROCK-JNK signaling axis. *Mol Cell*. 2004; 14:29. [PubMed: 15068801]
60. Montaner S, Sodhi A, Servitja JM, Ramsdell AK, Barac A, Sawai ET, Gutkind JS. The small GTPase Rac1 links the Kaposi sarcoma-associated herpesvirus vGPCR to cytokine secretion and paracrine neoplasia. *Blood*. 2004; 104:2903. [PubMed: 15231571]
61. Basile JR, Barac A, Zhu T, Guan KL, Gutkind JS. Class IV semaphorins promote angiogenesis by stimulating Rho-initiated pathways through plexin-B. *Cancer Res*. 2004; 64:5212. [PubMed: 15289326]
62. Armbruster BN, Li X, Pausch MH, Herlitze S, Roth BL. Evolving the lock to fit the key to create a family of G protein-coupled receptors potently activated by an inert ligand. *Proc Natl Acad Sci U S A*. 2007; 104:5163. [PubMed: 17360345]
63. Bhavsar PJ, Vigorito E, Turner M, Ridley AJ. Vav GEFs regulate macrophage morphology and adhesion-induced Rac and Rho activation. *Exp Cell Res*. 2009; 315:3345. [PubMed: 19715691]
64. Lin F, Baldessari F, Gyenge CC, Sato T, Chambers RD, Santiago JG, Butcher EC. Lymphocyte electrotaxis in vitro and in vivo. *J Immunol*. 2008; 181:2465. [PubMed: 18684937]
65. Safina A, Vandette E, Bakin AV. ALK5 promotes tumor angiogenesis by upregulating matrix metalloproteinase-9 in tumor cells. *Oncogene*. 2007; 26:2407. [PubMed: 17072348]

66. Percherancier Y, Berchiche YA, Slight I, Volkmer-Engert R, Tamamura H, Fujii N, Bouvier M, Heveker N. Bioluminescence resonance energy transfer reveals ligand-induced conformational changes in CXCR4 homo- and heterodimers. *J Biol Chem.* 2005; 280:9895. [PubMed: 15632118]

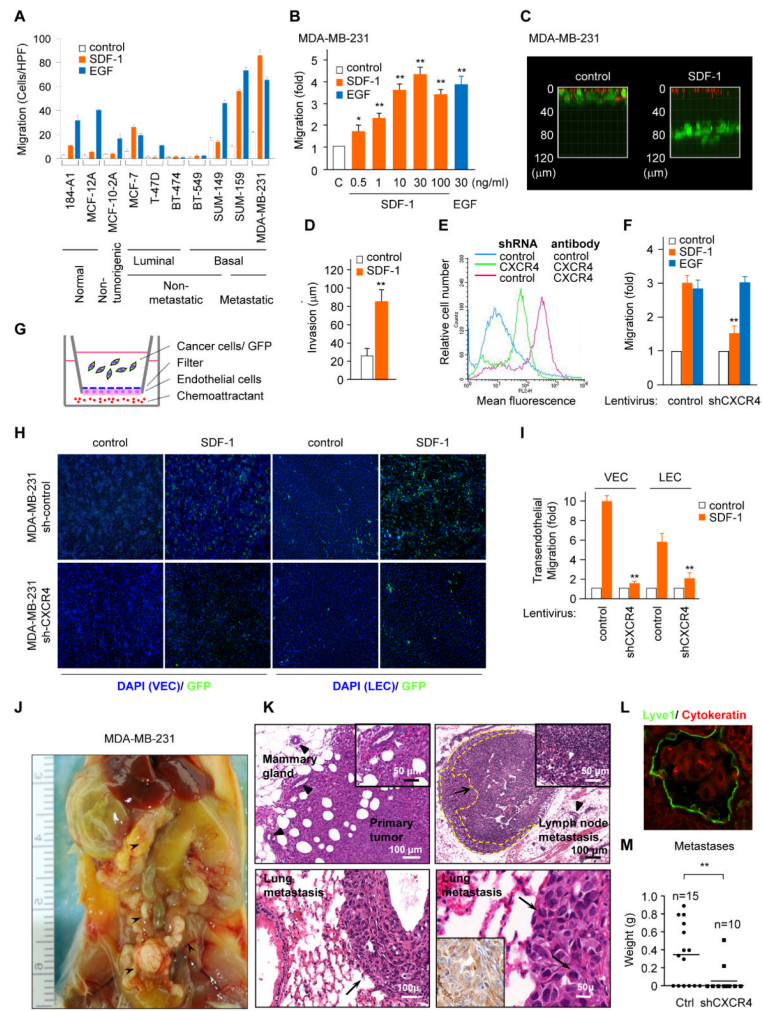


Fig. 1. CXCR4 mediates spontaneous metastatic spread of breast cancer cells

(A) Migration of nontransformed and malignant breast cell lines. Number of cells migrating per high power magnification frame (HPF) was recorded. Error bars, s.e.m. (B) SDF-1 induces the migration of MDA-MB-231 cells. Data represent the fold increase in cell migration with respect to the control cells (considered as a group). Error bars, s.e.m. * $p < 0.05$, ** $p < 0.01$ (C-D) MDA-MB-231 cells expressing GFP, 24 h of collagen gel invasion assay, representative images (C) and quantification (D). Error bars, s.e.m. ** $p < 0.01$. (E, F) Knocking down CXCR4 decreases MDA-MB-231 cell migration to SDF-1. FACS analysis was performed as described in Materials and Methods, using anti-CXCR4 mouse monoclonal antibody or isotypic control antibodies. Error bars, s.e.m. ** $p < 0.01$ with respect to cells infected with control lentivirus. (G) Schematic of the in vitro intravasation assay model system. (H, I) SDF-1 induces trans-endothelial migration of MDA-MB-231 cells by means of CXCR4. Images of transmigrated MDA-MB-231 cells expressing GFP after 24 h of in vitro intravasation assay (H), and quantification (I). Error bars, s.e.m. ** $p < 0.01$ with corresponding cells infected with control lentivirus. (J) Metastatic spread of MDA-MB-231 cells 40 days after orthotopic injection into the mammary fat pad of SCID/NOD mice. Arrow heads; metastatic sites. (K) H&E stain of MDA-MB-231 primary tumor and metastases. Upper left primary tumor growing within the mammary gland, and upper right regional (inguinal) lymph node metastasis (left of the yellow dotted line identified by the black arrow, and white arrow head in the insert). Inserts

are higher magnifications of the tumoral area. Black arrow head; mammary gland duct. Lower left; lung metastasis in low magnification showing the tumor mass (compact atypical cellular growth, black arrow) and the remaining lung parenchyma. Lower right; lung metastasis at a higher magnification, showing atypical feature of the compact mass of proliferating malignant cells (black arrow) and cytokeratin immunostaining of an adjacent histologic section indicating the epithelial nature of malignant cells (inset). **(L)** MDA-MB-231 cells within a lymphatic vessel. **(M)** Comparison of the weight of distant metastases between shRNA control and shRNA CXCR4 tumors. Horizontal bar, average; ** $p < 0.01$.

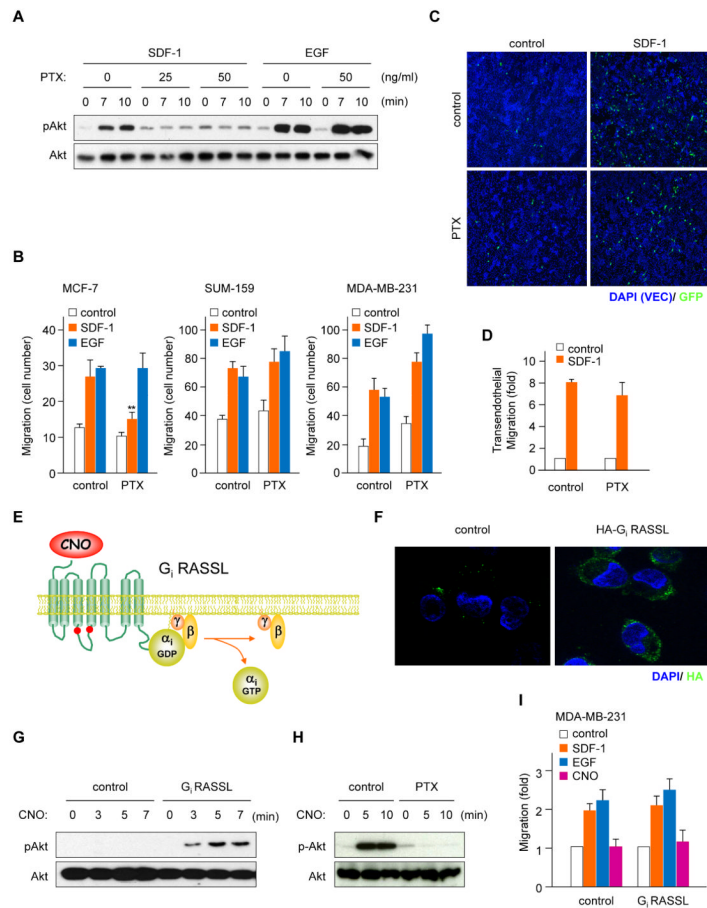


Fig. 2. SDF-1 can induce migration of metastatic breast cancer cells independent of PTX-sensitive heterotrimeric proteins of the $G\alpha_i$ family
(A) PTX inhibits the phosphorylation of Akt (Ser⁴⁷³) stimulated by SDF-1 in MDA-MB-231 cells, but **(B)** does not abolish the migration of MDA-MB-231 or SUM-159 cells to SDF-1. Error bars, s.e.m.; N=4 $**p<0.01$ compared with control cells stimulated by SDF-1. Blots are representative of 4 independent experiments. **(C, D)** $G\alpha_i$ activity is not required for trans-endothelial migration of MDA-MB-231 cells toward SDF-1. After pretreatment with PTX (50 ng/ml) overnight, in vitro transmigration activity was assessed. Error bars, s.e.m.; n=4 **(E)** Schematic of G_i RASSL (receptors activated solely by synthetic ligands). Clozapine-N-oxide (CNO) promotes the activation of G_i in cells expressing G_i RASSL. In red, graphical representation of the location of mutated amino acids that enable the response to CNO **(F)** Abundance of HA-tagged G_i RASSL in MDA-MB-231 cells. **(G)** CNO induces phosphorylation of Akt (Ser⁴⁷³) in MDA-MB-231 cells stably expressing G_i RASSL, which is inhibited by PTX **(H)**. Blots are representative of 4 independent experiments. **(I)** CNO fails to induce migration of MDA-MB-231 cells stably expressing G_i RASSL. Error bars, s.e.m.; n=4.

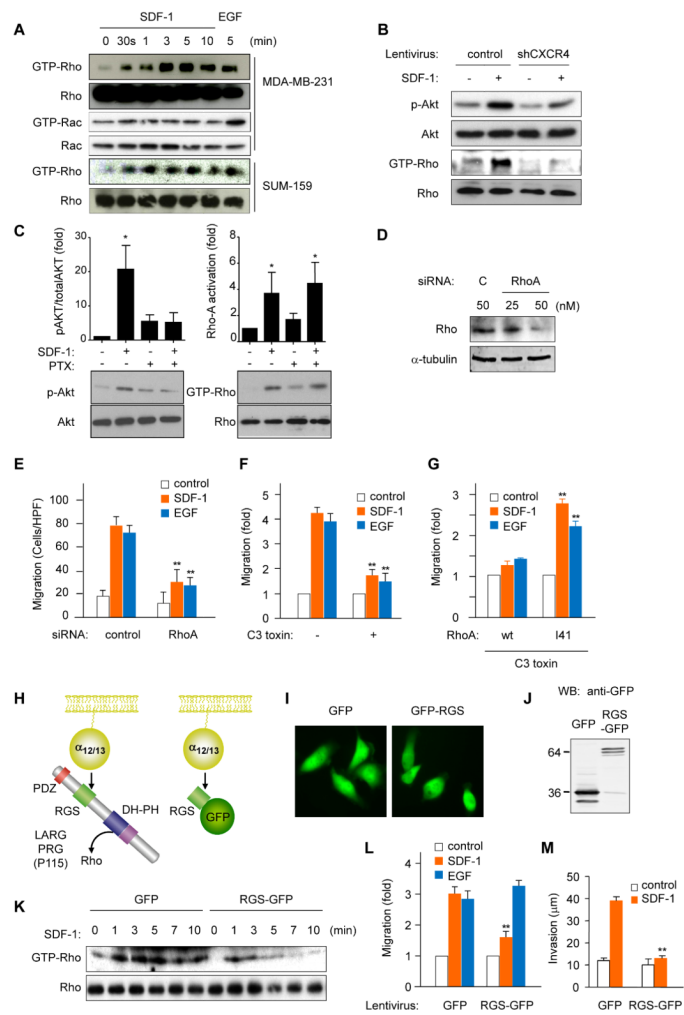


Fig. 3. CXCR4/ $G\alpha_{12/13}$ / Rho signaling axis is involved in migration of metastatic breast cancer cells

(A) Time course of Rho activation induced by SDF-1 in MDA-MB-231 and SUM-159 cells. (B) CXCR4 knockdown diminishes phosphorylation of Akt (Ser⁴⁷³) and Rho activation in response to SDF-1 in MDA-MB-231 cells. (C) Rho activation promoted by SDF-1 is independent of PTX-sensitive heterotrimeric G proteins of the $G\alpha_i$ family. Error bars, s.e.m. * $p < 0.05$ with respect to the corresponding cells not treated with SDF-1 (D) Knock down of RhoA by siRNA (E) inhibits the migration of MDA-MB-231 cells stimulated by SDF-1. The migration of MDA-MB-231 cells was examined 48 h after transfection of siRNA-control or siRNA-RhoA. Error bars, s.e.m. ** $p < 0.01$ compared with control cells stimulated by SDF-1 or EGF. (F) Treatment with C3 toxin inhibits the migration of MDA-MB-231 cells. ** $p < 0.01$. (G) C3 toxin fails to inhibit migration of MDA-MB-231 cells expressing C3 toxin insensitive mutant of RhoA, RhoA I41, but not RhoA wild type. Error bars, s.e.m. ** $p < 0.01$ with respect to the corresponding control cells. (H) Schematic of chimeric protein encoding RGS domain of PDZ-RhoGEF fused to GFP. (I, J) Expression of GFP or the GFP-RGS domain of PDZ-RhoGEF in MDA-MB-231 cells. (K) Inhibition of $G\alpha_{12/13}$ suppresses the activation of Rho by SDF-1 in MDA-MB-231 cells. (L-M) Inhibition of $G\alpha_{12/13}$ prevents cell migration (L) and invasion (M) induced by SDF-1. Error bars, s.e.m.; ** $p < 0.01$ with respect to the corresponding cells infected with GFP-lentivirus.

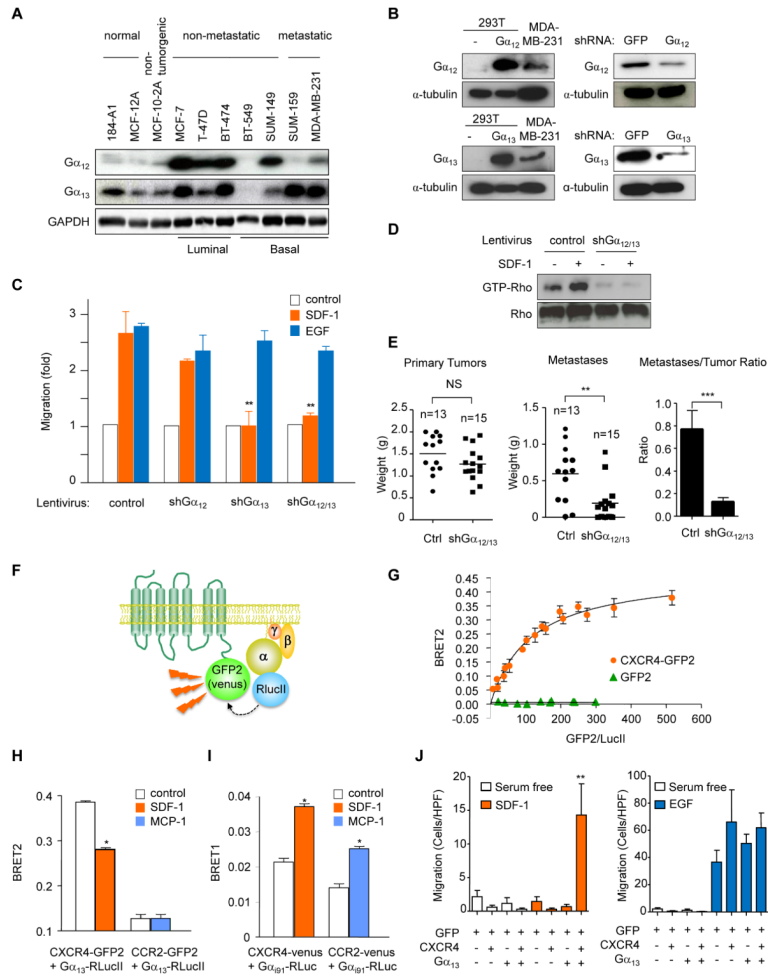


Fig. 4. CXCR4 signals through Gα_{12/13} in metastatic breast cancer cells

A. Abundance of Gα_{12/13} in human mammary cell lines. **(B)** Knock down of Gα_{12/13} by lentiviruses encoding Gα₁₂ shRNA or Gα₁₃ shRNA. **(C-D)** Knock down of Gα_{12/13} prevents migration of MDA-MB-231 cells stimulated by SDF-1 and inhibits Rho activation stimulated by SDF-1 in MDA-MB-231 cells. Error bars, s.e.m.; **p<0.01 with respect to the corresponding control shRNA lentivirus. **(E)** Scatter plot of the weight of primary tumors and metastatic sites, and the ratio between the weight of the metastases and primary tumors for each mouse, for MDA-MB-231 cells infected with lentivirus-control versus lentivirus-shRNA Gα_{12/13}. NS, no significant difference, **p<0.01 and ***p<0.001 compared with control. **(F)** Principle of bioluminescence resonance energy transfer (BRET). **(G)** Specificity of interaction between Gα₁₃-RlucII and CXCR4-GFP2. **(H)** A conformational change is promoted between Gα₁₃-RlucII and CXCR4-GFP2 but not between Gα₁₃-RlucII and CCR2-GFP2 by their cognate ligands. Error bars, s.e.m.; n=4 *p<0.05 compared with control in each group. **(I)** A conformational change is promoted between Gα_i-Rluc and CXCR4-venus and also between Gα_i-Rluc and CCR2-venus by their cognate ligands. Error bars, s.e.m.; n=4 *p<0.05 compared with control in each group. **(J)** SDF-1 induces the migration of HEK-293 cells co-expressing CXCR4 and Gα₁₃. In all cases, blots are representative of 3-4 experiments.

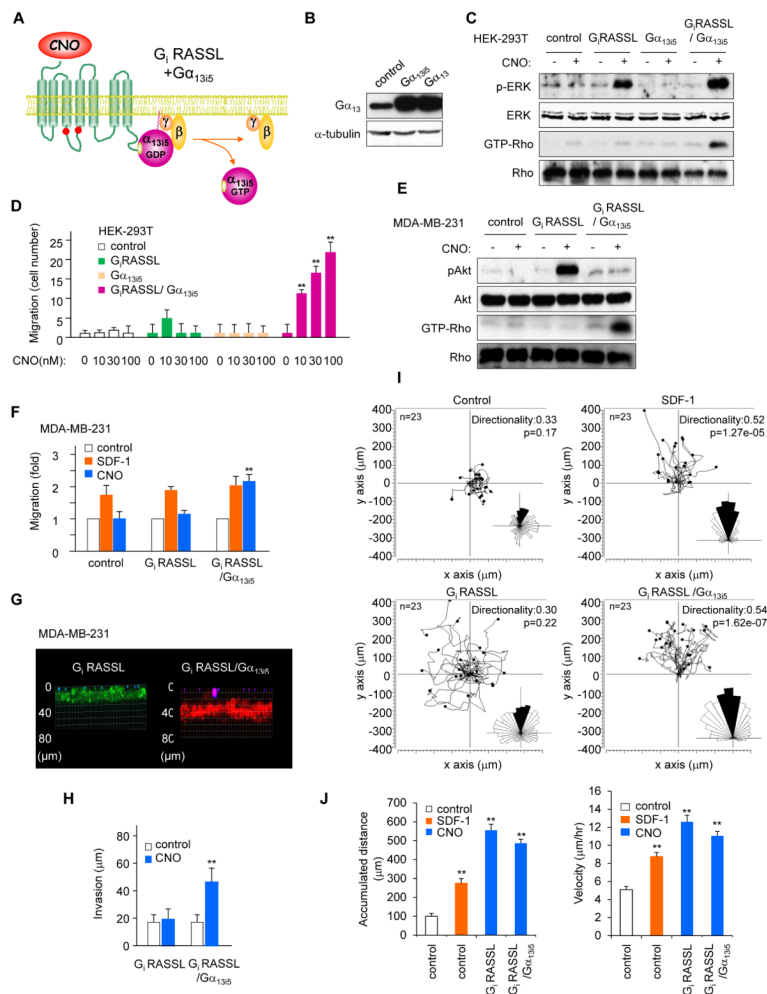


Fig. 5. A synthetic biology approach reveals a GPCR- $G\alpha_{13}$ -Rho signaling axis in breast cancer cell migration and invasion

(A) Schematic of cells co-expressing G_i RASSL and $G\alpha_{13i5}$. CNO promotes the activation of $G\alpha_{13}$ in cells co-expressing G_i RASSL and $G\alpha_{13i5}$. (B) Expression of $G\alpha_{13i5}$ in HEK-293T cells. (C) CNO induces activation of ERK and Rho in HEK-293T cells co-expressing G_i RASSL and $G\alpha_{13i5}$. (D) CNO induces the migration of HEK-293T cells co-expressing G_i RASSL and $G\alpha_{13i5}$. Error bars, s.e.m.; $n=4$ $**p<0.01$ compared to unstimulated cells. (E) CNO induces Rho activation in MDA-MB-231 cells co-expressing G_i RASSL and $G\alpha_{13i5}$. (F) CNO induces migration of MDA-MB-231 cells stably expressing G_i RASSL and $G\alpha_{13i5}$. Error bars, s.e.m.; $n=4$ $**p<0.01$ compared with cells without stimulation. (G-H) Invasion assay of MDA-MB-231 cells expressing G_i RASSL and GFP or G_i RASSL, $G\alpha_{13i5}$ and RFP after 24 h of collagen gel invasion, representative images (G) and quantification (H). (I-J) $G\alpha_{13}$ but not $G\alpha_i$ induces directional migration of MDA-MB-231; MDA-MB-231 cells or MDA-MB-231 cells expressing G_i RASSL or G_i RASSL with $G\alpha_{13i5}$ were seeded in the Chemotaxis μ -Slides as described in Material and Methods, and migration in response to either SDF-1 or CNO was recorded over 24 h. Individual cell movement ($n=23$) was tracked and represented in μm (I). The corresponding rose diagram was also plotted and shown in the inset. Graphs show the corresponding accumulated distance migrated for each cell (in μm) and their velocity (in $\mu\text{m/hr}$). (J), and

represent mean \pm s.e.m. ** $p < 0.01$ compared with cells without stimulation. In all cases, blots and images are representative of 3-4 experiments.

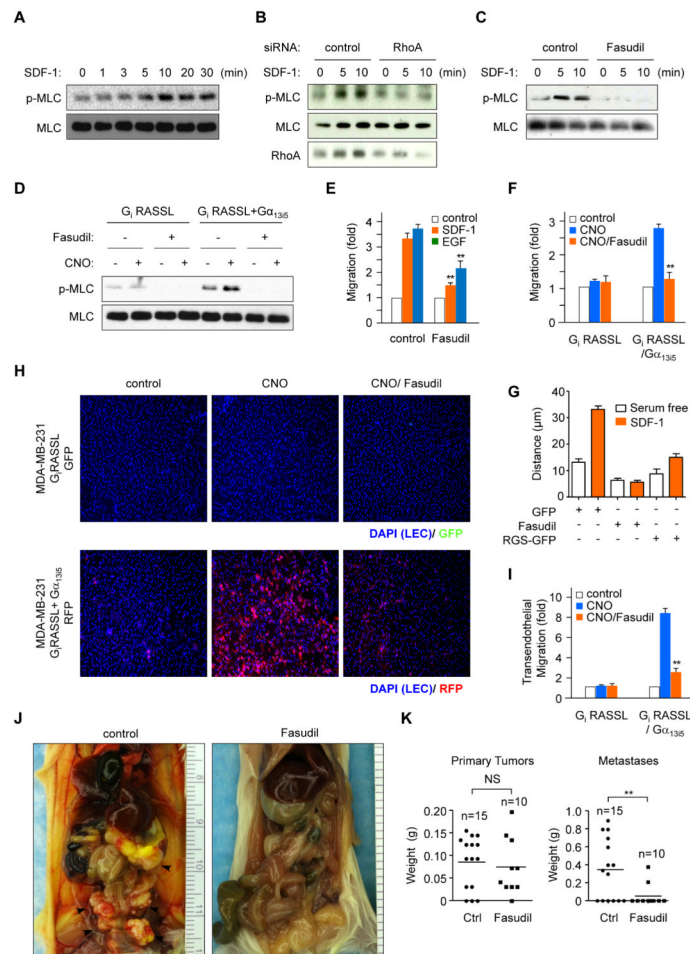


Fig. 6. Perturbing the CXR4-Rho-initiated signaling network provides a strategy for preventing breast cancer metastasis

(A) Time course of phosphorylation of MLC induced by SDF-1 in MDA-MB-231 cells. (B) Knock down of RhoA inhibits the activation of MLC stimulated by SDF-1. (C) Fasudil inhibits MLC phosphorylation stimulated by SDF-1. (D) Fasudil blocks the activation of MLC induced by CNO in MDA-MB-231 cells expressing both G_i RASSL and $G\alpha_{13i5}$. (E) Fasudil inhibits cell migration promoted by SDF-1. Error bars, s.e.m.; $n=4$ $**p<0.01$ compared with control cells stimulated by each stimulant. (F) Fasudil prevents migration of MDA-MB-231 cells co-expressing G_i RASSL and $G\alpha_{13i5}$ induced by CNO. Error bars, s.e.m.; $n=4$ $**p<0.01$ compared with control cells stimulated by each stimulant. (G) Fasudil treatment and RGS domain expression block SDF-1 induced invasion of MDA-MB-231 cells (H, I) CNO-induced lymphatic transendothelial migration of MDA-MB-231 cells stably expressing G_i RASSL, $G\alpha_{13i5}$, and RFP was blocked by Fasudil. Error bars, s.e.m.; $n=4$ $**p<0.01$ compared with control cells stimulated with CNO. (J) Fasudil inhibits metastatic spread of MDA-MB-231 cells injected into mammary fat pads of SCID/NOD mice. Arrow heads indicate metastases. (K) Scatter plot of weight of primary tumors and metastatic sites for control versus Fasudil treated group. NS, no significant difference and $**p<0.01$ compared with control. Western blots and images are representative of 3-4 independent experiments.